Article (refereed)

Clark, Douglas; Gedney, Nicola. 2008 Representing the effects of subgrid variability of soil moisture on runoff generation in a land surface model. *Journal of Geophysical Research*, 113 (D10111). doi:10.1029/2007/JD008940

Representing the effects of subgrid variability of soil moisture on runoff generation in a land surface model

Douglas B. Clark,

Centre for Ecology and Hydrology, Wallingford, Oxfordshire, United Kingdom

Nicola Gedney,

Hadley Centre for Climate Prediction and Research, Met Office, Joint Centre for Hydrometeorological Research, United Kingdom

Corresponding author: D.B.Clark, CEH Wallingford, Crowmarsh Gifford, Oxfordshire, OX10 8BB, United Kingdom. E-mail: dbcl@ceh.ac.uk

Abstract

Different representations of runoff generation processes were implemented in the MOSES land surface model which is used with mesoscale and global atmospheric models. The standard model was compared with versions in which runoff generation was described by parameterizations based on either the Probability Distributed Model (PDM) or modified forms of TOPMODEL, all of which used probability functions to describe the subgrid distribution of soil moisture. The model results were compared with observed streamflow in three catchments in southern France. After calibration, the PDM- and TOPMODEL-based parameterizations performed substantially better than the standard model. The TOPMODEL approach gave the best results through allowing a more responsive subsurface flow that contributed to peak flows and also better captured the slower changes during recessions. This approach was sensitive to uncertainty in the value of the topographic index. The PDM-based model only changed the calculation of surface runoff and retained the standard description of subsurface runoff, and this limited the possible improvement in performance. In principle the values of the new parameters can be determined from observations, but in practice calibration is likely to be required. However, for each new parameterization, a single set of parameter values was found that performed well in all catchments. The simulated soil moisture and surface heat fluxes during summer dry periods were affected by the choice of runoff parameterization.

1. Introduction

Land surface models for use in climate and NWP models have traditionally concentrated on the modeling of the radiative and turbulent fluxes that the atmospheric models require as boundary conditions. Further, there has been a tendency to develop relatively sophisticated one-dimensional models, in which the detail is in the vertical, while ignoring issues of horizontal heterogeneity within a gridbox [*Koster et al.*, 2000]. Both of these historical factors have tended to mean that the generation of runoff is treated very simply in land surface models. However, an unrealistic simulation of runoff can have detrimental effects on the simulation of evaporation [*Koster and Milly*, 1997] and hence on the partitioning of the surface energy fluxes. Furthermore, researchers are making increasing use of coupled models, linking atmosphere, land and ocean, in which runoff is a quantity of primary concern.

The processes governing the generation of runoff at the scale of a hillslope are complex and vary strongly with time and space. Runoff is often considered to be either surface runoff in which the water flows over the land surface, or subsurface runoff. Surface runoff can be divided into that generated by infiltration excess and saturation excess mechanisms. Infiltration excess runoff occurs when the rainfall rate is greater than that at which the water can infiltrate into the soil. Rainfall in excess of infiltration will then flow downslope as overland flow towards stream channels. Saturation excess overland flow occurs when rain falls onto saturated soil, often in valley bottoms and riparian areas. In either case, water that infiltrates the soil will eventually reach a layer of low permeability, at which point it becomes a downslope subsurface flow. In many catchments aquifers also contribute to the subsurface flow.

A coarse resolution land surface model cannot explicitly model the complexities of runoff generation within a catchment and instead aims to represent the major processes via subgrid parameterizations. A popular solution involves the use of probability distribution functions (pdfs) to represent subgrid variability, usually either a pdf of soil storage capacity [e.g., *Dumenil and Todini*,

1992; *Wood et al.*, 1992; *Liang and Xie*, 2001] or of topographic characteristics [e.g., *Famiglietti and Wood*, 1994; *Stieglitz et al.*, 1997; *Ducharne et al.*, 2000; *Chen and Kumar*, 2001; *Gedney and Cox*, 2003]. Both approaches aim to describe the impact of subgrid variability of soil moisture on runoff production.

In models that use a pdf of storage capacity, the distribution can be treated as a convenient functional form, as in the VIC model [*Wood et al.*, 1992], but can also be understood in terms of a statistical distribution of connected soil moisture stores and their overall response to rainfall, as in the Probability Distributed Model (PDM, [*Moore*, 1985].) The parameters of the distribution can be found from calibration of the overall runoff model, or an attempt can be made to infer them from physical characteristics of the catchment such as topography and soils [*Dumenil and Todini*, 1992; *Hagemann and Gates*, 2003]. The second type of model is based on TOPMODEL [*Beven and Kirkby*, 1979]. The tendency of each location within a catchment to be saturated is estimated using a topographic index λ, defined as $\lambda = \ln(a / \tan\beta)$, where a is the area draining to this location per unit contour length and $\tan\beta$ is the slope of the land surface. The pdf of λ is used to calculate the overall saturated area. *Famiglietti and Wood* [1994] combined TOPMODEL with a land surface model, while *Stieglitz et al.* [1997] developed a simpler version of TOPMODEL for climate models and applied the equations to the single soil column that represented the average state of the catchment.

The increasing availability of relatively high resolution fields of terrain height has meant that parameterizations based on the TOPMODEL approach have been implemented in several models [*Ducharne et al.*, 2000; *Chen and Kumar*, 2001; *Habets and Saulnier*, 2001; *Warrach et al.*, 2002; *Niu and Yang*, 2003]. Although TOPMODEL is physically-based, many of the assumptions only hold in certain catchments or at certain times [*Beven*, 1997] and must be regarded as poorer approximations at the scale of climate models.

Habets and Saulnier [2001] compared the VIC and TOPMODEL-type approaches and found little difference in results, but a study by *Warrach et al.* [2002] found in favor of TOPMODEL.

Other studies have compared a TOPMODEL-type approach with simpler schemes and found that the topographic approach gave better estimates of runoff, with improved subsurface flow again being important [*Stieglitz et al.*, 1997; *Chen and Kumar*, 2001].

The land surface model used in the present study is the Met Office Surface Exchange Scheme (MOSES, *Essery et al.*, 2003). MOSES has been used with both PDM [*Blyth*, 2002; *Boone et al.*, 2004] and TOPMODEL-type parameterizations of runoff [*Gedney and Cox*, 2003], but a comparison of these has not previously been attempted. The present work was motivated by the desire to identify which parameterization better represented observed river flows and complements previous studies by testing a range of model formulations on the same data and presenting sensitivity studies.

The remainder of this paper is arranged as follows: Section 2 describes the model and data used, and Section 3 presents results with the standard model. Sections 4 to 6 give the results of alternative parameterizations, before Section 7 provides an overall comparison of the models.

2. Model, Data and Methodology

2.1. Description of the Model

Details of MOSES can be found in *Essery et al.* [2003], while a few key features will be highlighted here. The soil is divided into vertical layers and moisture fluxes between layers are modeled using a finite difference approximation to the Richards' equation, with the soil hydraulic characteristics following *Clapp and Hornberger* [1978]. Water drains from the bottom of the soil column at a rate equal to the hydraulic conductivity of the bottom layer. Surface runoff is generated by the infiltration excess mechanism following *Dolman and Gregory* [1992], assuming an exponential distribution of point rainfall rate across the fraction of the catchment where it is raining. Infiltration excess runoff is relatively rare on the gridscale of a climate model, and most runoff from

MOSES is via drainage. Alternative parameterizations for runoff generation were introduced, as described below, but all other aspects of the model, including the calculation of infiltration excess runoff, were unchanged.

2.2 PDM-based Runoff Scheme

The Probability Distributed Model (PDM) is described by *Moore* [1985] and *Moore and Bell* [2002]. In PDM, the distribution of soil storage capacity within a catchment is modeled by a pdf. In this study each catchment was modeled as a single gridbox and the following development uses the gridbox mean storage S. As precipitation is added to the soil stores, the smaller stores are the first to saturate. The fraction of the gridbox that is saturated can be shown to be

$$f_{sat} = 1 - \left(1 - \frac{S - S_0}{S_{\max} - S_0}\right)^{\frac{b}{b+1}}$$

where S_0 is the minimum storage below which there is no surface saturation, S_{max} is the maximum possible gridbox storage (at saturation) and b is a shape parameter. The interpretation of the value of b in terms of the shape of the pdf is discussed by *Moore* [1985]. Subsequent precipitation on the saturated fraction of the catchment generates surface runoff, which is calculated as shown in the Appendix. Surface runoff can be generated before the entire catchment is saturated, and the amount of runoff depends in part on the antecedent soil moisture. Note that if S_0=0, PDM reduces to the form used in several models, including VIC. MOSES_PDM calculated saturation excess surface runoff following PDM and introduced three new parameters. Available data were used to prescribe S_{max} (see Section 4.1), leaving b and S_0 to be calibrated.

2.3. TOPMODEL-based Runoff Scheme

For details of the theory underlying TOPMODEL, see *Beven and Kirkby* [1979] and *Sivapalan et al.* [1987]. In TOPMODEL, the spatial variability of soil moisture is parameterized in terms of the spatial distribution of λ. The saturated hydraulic conductivity, K_s, is assumed to decrease with depth beneath the surface (z) as

$$K_s(z) = K_{s0} e^{-fz}$$

where K_{s0} is the saturated conductivity at the soil surface and f is a decay parameter. *Chen and Kumar* [2001] introduced an anisotropy factor, α, to account for differences of K_s in the vertical and horizontal directions, $K_{sx} = \alpha K_{sz}$ (hereafter, the subscript z is dropped and K_s refers to the vertical direction). Lateral subsurface flow (known as baseflow) occurs at a rate given by

$$R_b = \frac{\alpha K_{s0}}{f} e^{-\Lambda} e^{-f z_w} \qquad (1)$$

where Λ and z_w are the catchment averages of λ and the depth to the water table respectively. Given z_w, the saturated fraction of the catchment can be calculated from the pdf of λ [*Beven and Kirkby*, 1979]. For a rainfall rate P (net of interception), saturation excess surface runoff is calculated as

$$R_s = f_{sat} P .$$

TOPMODEL was implemented in the current work following the approach of *Stieglitz et al.* [1997], and this version of the model was called MOSES_TOP. There was no drainage though the bottom of the soil column and the depth to water table was diagnosed using an equilibrium assumption for the soil water at each timestep, following *Chen and Kumar* [2001]. The baseflow was partitioned between layers beneath the water table according to the transmissivity of each layer. Some previous studies [e.g. *Chen and Kumar*, 2001] calculated evaporation separately for the

saturated and unsaturated fractions of the catchment, but MOSES_TOP used the gridbox average soil moisture when calculating transpiration.

MOSES_TOP involved several new parameters. Available data were used to prescribe K_{s0} (see Section 5.2) and the two parameters used to describe the pdf of λ, leaving f and α to be calibrated.

2.4 The Study Area, Data Sources and Methodology

This study focuses on three subcatchments of the Rhône basin in southeast France that were also considered as part of the Rhône-AGG experiment [*Boone et al.*, 2004]. Brief details of each are given in Table 1, while their locations can be seen in Fig.1 of *Boone et al.* [2004]. All of the catchments were relatively wet, with annual precipitation in excess of 1200mm and relatively little snowfall.

Land surface and soil properties were specified as in the Rhône-AGG experiment. Simulations with MOSES and MOSES_PDM used four soil layers, with total depth equal to the observed catchment-average (typically 2 to 3 m). Simulations with MOSES_TOP used the same top four layers, but added two deeper layers to take the bottom of the soil column to 10m. Each catchment was represented as a single grid box. The areas of the catchments correspond to a length scale of 30-50km, which is sufficiently large to include substantial subgrid variability of surface and soil characteristics. The model was driven by 3-hourly, catchment-average meteorological conditions (see *Boone et al.*, 2004).

Model performance was assessed by comparing simulated and observed streamflow. Only the treatment of runoff in the model was altered, hence some of the error in simulations could be a result of deficiencies in other parameterizations. MOSES has no representation of runoff routing in streams, but all parts of the three catchments are closer than one day's travel to the catchment outlet (A.Boone, personal communication, 2003) and the need for explicit consideration of flow routing was avoided by comparing three-day averages of modeled runoff and observed streamflow.

The model was spun up by repeatedly simulating the period August 1985 to July 1986 until a quasi-steady state was obtained. Each integration was then continued for three years to July 1989. Calibration used data for August 1986 to July 1987, and August 1987 to July 1989 was used as a validation period to assess the model performance outside the calibration period.

The statistic that is used in most of the analysis that follows is the modeling efficiency [*Nash and Sutcliffe*, 1970], defined as

$$E = 1 - \frac{\sum_{i=1}^{N}(M_i - O_i)^2}{\sum_{i=1}^{N}(O_i - \overline{O})^2}$$

where M_i denotes a modeled value at time i, O_i an observed value, an overbar indicates the average and the sum is over N times. E is a measure of the extent to which the model is an improvement over using the average observed flow, with a perfect model giving E=1. The quadratic nature of E means that it is sensitive to outliers, and mistimed peaks result in substantially lower values. The model bias ($\overline{M} - \overline{0}$) and mean absolute error (MAE; $1/N \sum_{i=1}^{N}|M_i - O_i|$) are also used below.

Calibration was performed by specifying a set of values for each parameter, and running the model for all possible combinations of values. This was considered to give reasonable estimates of the optimal parameter values because the response surfaces were relatively smooth.

3. Simulations with MOSES

Summary statistics for simulations with MOSES are given in Table 2. On average, MOSES produced more runoff than observed, with a large wet bias in the Ognon. The bias in the Ognon could be reduced by calibrating the soil hydraulic properties, but a substantial bias remained and it was decided to use the soil properties as given for all catchments.

Precipitation and observed and modeled streamflow for one year in the Ain are shown in Fig.1a and b. The modeled flow was dominated by drainage (over 99% of the total), with negligible

surface runoff. (All runs in the present study produced small amounts of infiltration excess runoff.) The modeled peaks were generally too low and late, consistent with the fact that runoff was largely generated by drainage through the bottom of the soil column, while there was too much flow during recessions. Qualitatively similar results were obtained for all catchments.

4. Simulations with MOSES_PDM

4.1 Calibration of MOSES_PDM

The pdf of soil storage capacities used in MOSES_PDM is described by the shape parameter b and the storage parameters S_0 and S_{max}. S_{max} was set to $\theta_{sat}\, z_{pdm}$, where θ_{sat} is the volumetric moisture content at saturation. z_{pdm} is the depth over which soil moisture is considered for PDM and was taken to be 1m. The model was calibrated for each catchment by varying b between 0 and 10, and S_0/S_{max} between 0 and 1. The optimal parameter values are given in Table 3, while Fig.2 illustrates the E values. In this figure, MOSES and then three runs of MOSES_PDM are shown for each catchment (the runs with TOPMODEL are considered later). The MOSES_PDM runs are: (1) PDM_0: the best calibrated model with the constraint that S_0 was zero (2) PDM_calib: the best calibrated model for each catchment (3) PDM_best: the single pair of parameter values that, when used for all catchments, gave the best results averaged over the three catchments. In the remainder of this work, such a "best" set of values is termed a "best overall" set. The final group in this figure, labeled "average", shows the efficiency averaged over the three catchments. (Note that in Fig.2, E for PDM_calib in the Ognon is less than that for the best overall model because E is given for the validation period, not the calibration period.)

For the Ain and Ardeche, MOSES_PDM performed substantially better than MOSES. The final set of results in Fig.2 confirms that, on average, MOSES_PDM performed substantially better than MOSES. On average, restricting the model to S_0=0 (PDM_0, as used in VIC) still resulted in considerable improvement over MOSES, but non-zero values of S_0 gave better results. It was not

surprising that adding a parameter allowed better simulations, but non-zero values of S_0 also make physical sense, as discussed below. The best overall model (PDM_best) had parameter values S_0/S_{max}=0·75, b=10.

The modeled streamflow for the Ain, using the "best overall" parameters, is shown in Fig.1c. Comparison with the MOSES results (Fig.1b) shows that the timing of the peaks was better simulated by MOSES_PDM, but the peaks remained low. Fig.1d shows that subsurface drainage was dominant (over 75%), with saturation excess surface runoff contributing to the peaks. MOSES_PDM also showed excessive flow during recessions, consistent with the fact that drainage was simulated in the same way as by MOSES. The lower infiltration with PDM was largely balanced by reduced drainage, and total runoff was very similar between runs with and without PDM.

4.2 Sensitivity of MOSES_PDM

The sensitivity of MOSES_PDM to parameter values is illustrated by the whiskers shown next to PDM_best in Fig.2. These show the effects of varying S_0 by ±10% about its value in the best overall model. The sensitivity to b was too small to be plotted in this way. In every catchment, the sensitivity was sufficiently small as to mean that the "best overall" parameters gave better results than MOSES.

These results are best interpreted with the help of Fig.3, which shows the response surface for the Ain. Small values of S_0 meant that nearly every rainfall event would result in surface runoff, in which case b<1 was best (relatively more larger stores – see *Moore* [1985]) since this gave a smaller saturated fraction and reduced the size of the runoff peaks. The highest efficiency was found with S_0/S_{max} ~0.7, meaning that no saturation excess runoff was generated until the soil was 70% saturated. This gave good results by generating surface runoff to augment large peaks of streamflow when the catchment was very wet, while not generating any surface runoff over a drier catchment. This seems reasonable, since for many dry catchments one would expect there to be

little or no saturated area (outside channels) and a rainfall event could all be absorbed by the soil without any surface runoff. S_0/S_{max} ~0.7 favoured larger values of b (relatively more small stores) since these tend to give more runoff during the peak flows. As small b or large S_0 increased the ratio of subsurface to surface runoff, the best runs in Fig.3 were all dominated by subsurface flow.

The simpler parameterization with S_0=0 was very sensitive to b and an advantage of allowing larger values of the threshold S_0 was that this sensitivity was reduced, particularly for S_0/S_{max} ~0.7. In all catchments the response surface of E showed slow variation around the optimum. This meant that the simulation for a given catchment was not critically dependent upon the exact parameter values and, more importantly, it was possible to identify a "best overall" set of parameters.

4.3 A Priori Estimation of Parameter Values for MOSES_PDM

The values of b can be set by calibration [e.g. *Warrach et al.*, 2002] or may be considered constant over all catchments [e.g. *Habets et al.*, 1999]. Other studies have attempted to link the parameters of PDM-like models to physical characteristics. *Dumenil and Todini* [1992] calculated b as a simple function of the subgrid standard deviation of elevation, so that hilly terrain gave a larger value of b and would tend to give more runoff. *Hagemann and Gates* [2003] used a soil dataset to characterize the subgrid distribution of soil storage and fitted a pdf to this.

In the present work, the relatively low sensitivity of MOSES_PDM to parameter values meant that both methods for estimating values *a priori* gave reasonable results. However, better results were obtained by using a single set of calibrated parameters for all catchments. Moreover, both *a priori* methods are potentially sensitive to the resolution of the data used. More catchments would need to be studied to determine if there is any useful relationship between parameter values and catchment characteristics, and in the meantime we propose to use the "best overall" parameters for all catchments.

5. Simulations with MOSES_TOP

5.1 Estimation of parameters of the topographic index

The pdf of λ for each catchment was modeled as a two-parameter gamma distribution, using the HYDRO1K global dataset (http://edc.usgs.gov/products/elevation/gtopo30/hydro) to calculate the mean (Λ) and standard deviation (σ_λ) of λ for each catchment. These statistics are sensitive to the resolution of the elevation data used [e.g., *Wolock and Price*, 1994; *Zhang and Montgomery*, 1994; *Saulnier et al.*, 1997; *Kumar et al.*, 2000; *Wolock and McCabe*, 2000; *Ibbitt and Woods*, 2004; *Bormann*, 2006; *Pradhan et al.*, 2006]. Generally Λ decreases as finer resolution data are used, while *Kumar et al.* [2000] showed that σ_λ also decreases. For global or other large-scale applications, data on a 1 km grid (such as HYDRO1K) are often used, but *Ibbitt and Woods* [2004] suggested that data at much greater resolution would be required to estimate the "true" value. Figure 4 summarises the results of several published estimates of how Λ varies with grid size. These studies have considered different locations and there is considerable scatter between the results. In general there appears to be a modest decrease of Λ down to grid sizes of the order of 100m, with a much larger rate of decrease for smaller grid sizes. *Ibbitt and Woods* [2004] and *Pradhan et al.* [2006] have considered how a theory for downscaling might be developed, but as yet there is no robust method with which to adjust Λ.

Far from it being the case that Λ has a value that can be defined via readily-available topographic data, the value of Λ is highly uncertain. Some studies authors have acknowledged the scale-dependence of Λ, and have attempted to correct for it. For example, *Chen and Kumar* [2001] downscaled from 1km to 90m, while *Niu and Yang* [2003] downscaled from 1km to 100m. However, Fig.4 suggests that estimates of Λ may continue to vary to much smaller scales. This uncertainty in Λ is important because, as will be shown later, variations in Λ of this size can result in substantially different model performance.

In the current work, the simple relationship $\Lambda = \Lambda_{1000} - 5$ was to used to calculate Λ from the HYDRO1K value of Λ_{1000}. This arbitrary rule was intended to capture some of the behaviour shown in Fig.4 as the grid size decreases from 1km to of the order of 10m. Implicit in this approach was the assumption that there is a "correct" value of Λ, which might be determined with high resolution data. This gave values of 7·6, 6·0 and 7·3 for the Ain, Ardeche and Ognon respectively. No attempt was made to account for the effect of data resolution on σ_λ. The calculated values of Λ are clearly subject to large uncertainty and the sensitivity of the models to the value of Λ is explored below.

5.2 Calibration of MOSES_TOP

Existing global datasets generally do not contain enough information to specify a vertical profile of K_s. Previous studies have adopted a variety of approaches to relate a given value of K_s to a surface value (K_{s0}) and the decay parameter f [*Stieglitz et al.*, 1997; *Chen and Kumar*, 2001; *Warrach et al.*, 2002; *Decharme et al.*, 2006]. For the current work, the value of K_s that was provided for each catchment was assumed to be the average down to a depth of 2m (results were not particularly sensitive to this depth). The value of K_{s0} was then calculated for each value of f. This resulted in relatively large values of K_s close to the surface, consistent with the existence of macropores and less compacted soil in these layers.

MOSES_TOP was calibrated by varying f over the range 1 to 9, and α over the range 1 to 100. This range of α was motivated by results in the literature. *Chen and Kumar* [2001] used a value of 2000, found by calibration, while *Niu and Yang* [2003] used values in the range 10-20. In a review of published results, largely from laboratory and pumping tests, *Kumar* [2004] noted values in the range of 0·4 to 562, with most studies suggesting a maximum of less than 100.

The calibrated parameter values are shown in Table 4. Again, it was possible to identify a single set of parameters that gave good results in all catchments: f=3·0, α=100. The values of f found by calibration were of the order of 3-4 and were broadly consistent with those found in previous modeling studies [*Stieglitz et al.*, 1997; *Chen and Kumar*, 2001; *Warrach et al.*, 2002; *Niu*

and Yang, 2003; *Decharme et al.*, 2006], and certainly within the wide range found by *Beven* [1982] in observations. The last line in Table 4 shows that the decision to restrict α to values of 100 or less did not drastically affect the results.

The last two bars in each section of Figure 2 represent *E* for MOSES_TOP calibrated for each catchment, and MOESES_TOP with "best overall" parameters. Simulations with MOSES_TOP were better than those with MOSES in all catchments, particularly the Ain and Ardeche. The simulated hydrograph shown in Fig.1e confirms that the timing and size of peak flows were well captured by MOSES_TOP, and recessions were also generally well matched. Figure 1f shows that the optimal parameters resulted in runoff that consisted largely of subsurface flow (84%). Although MOSES and MOSES_TOP were both dominated by subsurface flow, the more rapid variations of MOSES_TOP compared much more favorably with the observed streamflow.

5.3 Sensitivity of MOSES_TOP

The sensitivity of MOSES_TOP to the values of *f* and α is illustrated for the Ain in Fig.5a. With *f*=3, using α=1 gave simulations that were much too 'flashy' due to low baseflow and a large saturated fraction. A better match to observations was found with larger values of α which gave increased baseflow and smaller saturated fraction. Sensitivity to α was small for α≥200, but was much greater when α was in the range suggested as physically plausible, namely α~100. (This result is sensitive to the value of Λ – see below).

Larger values of *f* gave faster decrease of K_s with depth, which tended to produce a higher water table (i.e. closer to the surface) and greater baseflow. With α=2000, using *f*=1 gave a lower water table but low flows were too high and peaks too low. *f*=8 meant the low flows were too small, but the column could wet up quickly, giving large saturated fraction and peak flows that were too great. Hence an intermediate value of *f* gave best results (Fig.5a).

The model's sensitivity to Λ is summarized in Fig5b, which shows E as a function of $\Delta\Lambda_{1000}$, the amount subtracted from Λ_{1000}. Increasing Λ decreases baseflow by Eq.1 and gives a higher

water table. Figure 5b shows that for f=3, α =1000, sensitivity to Λ was low for values of $\Delta\Lambda_{1000}$<-2. For α =100, $\Delta\Lambda_{1000}$<-5 was required and the standard runs ($\Delta\Lambda_{1000}$=-5) lay in this regime. For α=1, $\Delta\Lambda_{1000}\approx$-10 (*c.f.* average Λ_{1000}=11.6) was required to get similarly large E values. This parameter interdependency is considered further in the next section.

5.4 Interplay Between Parameters of MOSES_TOP

Previous studies with TOPMODEL noted that the same runoff could be obtained in simulations with different values of Λ, as long as the transmissivity values were adjusted appropriately [*Franchini et al.*, 1996; *Saulnier et al.*, 1997]. For TOPMODEL, the problem was often approached in terms of how to adjust Λ so that values of K_{s0} found by calibration could be applied in models of different gridbox size. In the present work, K_{s0} was set using soil data and in that sense was removed from the problem. However, the introduction of α means that the terms α and $e^{-\Lambda}$ in Eq.1 can show similar compensation, assuming the same depth to water table. That is, considering two simulations with identical values of f, K_{s0} and z_w, but the first uses (Λ_1, α_1) while the second has the distinct values (Λ_2, α_2), Eq.1 shows that the same runoff will result if

$$\alpha_2 = \alpha_1 \exp(\Lambda_2 - \Lambda_1) \quad (2).$$

Franchini et al. [1996] show that the assumption of equal z_w is generally valid for TOPMODEL, and comparisons of simulations confirmed that Eq.2 was also a good approximation for MOSES_TOP across a wide range of parameter space. This compensation between parameters explains the family of curves seen in Fig.5b, with the maximum E found at smaller Λ as α decreases. The large values of α that were found by calibration in *Chen and Kumar*[2001] may, in part, have been necessary to adjust for insufficient downscaling of Λ..

The TOPMODEL-type parameterization used here is, in some senses, over-parameterized. The values of α and Λ are highly uncertain, and there is compensation between them. This motivated *Niu and Yang* [2003] to develop an alternative parameterization, which is described in Section 6.2 below.

6. Alternative TOPMODEL-type Parameterizations

The previous section established that a parameterization based on TOPMODEL gave the best simulations of runoff. TOPMODEL has been implemented in a variety of ways in land surface models. This section considers the sensitivity of our model to aspects of the parameterization.

6.1 Description of MOSES_TOPgc

Gedney and Cox [2003] implemented TOPMODEL in MOSES assuming that the exponential profile of K_s only held below the bottom of the standard soil model at 3m. The standard soil layers were augmented by a deeper layer in which a simplified treatment of soil water was used. In the present work, tests showed that this model was relatively unresponsive because the soil moisture in the deep layer was assumed to all lie below the water table, with a dry layer between this and the bottom of the standard soil model. To produce a more realistic response of the water table, the moisture distribution in the deep layer was taken to be in equilibrium with the drainage at the bottom of the standard soil model. This modified version was used here as MOSES_TOPgc

MOSES_TOP and MOSES_TOPgc differed in terms of the vertical variation of K_s and in the number of soil layers. Both required the parameters f and α to be calibrated, and Λ was set to Λ_{1000}-5.

6.2 Description of MOSES_TOPsim

Niu and Yang [2003] and *Niu et al.* [2005] described a model called SIMTOP that was inspired by the form of TOPMODEL, but was considered simpler. In the present study, this model was implemented as MOSES_TOPsim. The saturated fraction was calculated as

$$f_{sat} = f_{\max} \exp(-cfz_w)$$

where f_{max} is the saturated fraction when the mean depth to the water table is zero, and can be found as the fraction of the catchment with $\lambda \geq \Lambda$. The value of c was found by fitting an exponential distribution to that part of the pdf with $\lambda \geq \Lambda$, where an exponential often gives a good fit [*Woods and Sivapalan*, 1997; *Niu et al.*, 2005]. Subsurface runoff is calculated as

$$R_b = R_{b\max} e^{-fz_w} \quad (3)$$

where the parameter R_{bmax} is the subsurface runoff when the depth to the water table is zero. *Niu et al.* 2005] considered that the advantage of using Eq.3 rather than Eq.1 to calculate R_b was that the single, entirely calibrated term R_{bmax} replaced the product of α, K_{s0}, $1/f$ and $e^{-\Lambda}$.

MOSES_TOPsim was implemented with four soil layers down to the depth given in the soil dataset. In all other respects, MOSES_TOPsim followed MOSES_TOP.

6.3 Calibration of MOSES_TOPgc and MOSES_TOPsim

Table 4 shows that, after calibration, MOSES_TOPgc performed slightly better than MOSES_TOP. MOSES_TOPgc, for which K_s decays only in the deep layer, favored higher values of f which reduced K_s more quickly in the deep layer. Sensitivity to parameter values was also similar in each model (not shown). In summary, the modifications of *Gedney and Cox* [2003] appear to have largely retained the functioning of a model based on *Stieglitz et al.* [1997].

MOSES_TOPsim was calibrated by varying f in the range 0 to 8, and R_{bmax} over $0{\cdot}5\text{-}10\times10^{-4}$ kg m^{-2} s^{-1}. Table 4 shows that this version of the model could be calibrated to give statistics very similar to those of MOSES_TOP and MOSES_TOPgc. The optimum value of f =3 was similar to that found by *Niu et al.* [2005], while R_{bmax}=1.0×10^{-3} kg m^{-2} s^{-1} was slightly larger, although different catchments were studied. Again, the optimum parameters meant more subsurface runoff (89%) than surface runoff. By equating Eq.1 and Eq.3, using f=3 and other values appropriate to the

catchments, we find that R_{bmax}=1.0×10^{-3} kg m^{-2} s^{-1} is equivalent to α≈250 on average, which is comparable to the values used for MOSES_TOP.

7. Intercomparison of models

7.1 Runoff

The ability of each model to simulate the observed streamflow is summarized in Table 5, while values of *E* can be compared in Fig.2. In Table 5, values shown are for the best overall parameter values for each model (that is, the parameter values that when used in all catchments gave the largest *E* averaged over all catchments). For *E* and *MAE*, all of the parameterizations scored better than the original MOSES. The best models were MOSES_TOPgc and MOSES_TOPsim. Similar results held for the bias, although MOSES_TOP actually increased the bias. The fact that all statistics tended to improve while calibration considered only *E*, increases our confidence that the new models are a real improvement. The sensitivity of the calibrated models to changes in parameters around the optima was also broadly similar – as shown in Fig.2 for MOSES_PDM and MOSES_TOP.

In view of the remaining uncertainties, and the likelihood of variations between catchments, all the TOPMODEL-type parameterizations can be considered to belong to a "top group" that performed best. The fact that all the TOPMODEL-type formulations can be calibrated to perform similarly is not surprising, given that the process representation is very similar in each. The TOPMODEL approach gave subsurface runoff that could vary more rapidly than the formulation used in MOSES and MOSES_PDM. The longer term behavior in recessions was also captured better, as shown by the autocorrelation of streamflow, which is shown for the Ain in Fig.6. That is, the alternative formulation of subsurface flow in the TOPMODEL-type models was crucial to their superiority, with a lesser contribution from the saturation excess surface flow (although the two are

intimately linked). At the scale of these catchments (>1000 km^2) it is quite possible that, outside of the stream network, subsurface flow is dominant.

While the TOPMODEL group introduced alternative ways of calculating both surface and subsurface runoff, MOSES_PDM represented an intermediate class in which only the calculation of surface runoff was altered from MOSES. Consistent with this, results were intermediate between those of MOSES and the TOPMODEL group, although *E* values were close to those of the latter. For MOSES_PDM, the inclusion of saturation excess surface runoff during rain events greatly improved the simulation of peak flows. The contribution of surface runoff meant MOSES –PDM showed more variation than MOSES over timescales of a few days, but at longer timescales the curve for MOSES_PDM relaxes back onto that for MOSES (Fig. 6), because both simulated drainage in the same way. It seems likely that the performance of MOSES and MOSES_PDM could be improved by altering the representation of subsurface drainage (and calibrating any additional parameters), but this was not investigated here.

The new parameterizations tended to perform better than MOSES in the Ain and Ardeche, but their superiority was less marked in the Ognon. In the Ain and Ardeche, the correlation of precipitation and streamflow was greatest when streamflow was lagged by one day (not shown). In the Ognon, the maximum correlation occurred with a lag of 3 days. This simple result could be influenced by several factors, but suggests a difference between the catchments. The nature of this difference is unknown, but possible factors are that the Ognon has extensive limestone and karst [*BRGM*, 1970, although some is also present in the Ain], and is also the flattest catchment studied.

7.2 Soil water and energy balance

The catchments studied here were relatively wet and the various parameterizations tested had relatively little impact on the total runoff or evaporation: soil evaporation was rarely limited by moisture availability and changes in surface runoff were largely balanced by opposite changes in

the subsurface. However, moisture stress became more important in drier summers and then the calculated turbulent fluxes were sensitive to the parameterization of subgrid variability. Figure 7a show the soil wetness (expressed as a fraction of saturation) in the top 1m of soil for the Ardeche catchment during part of 1986. (MOSES, MOSES_PDM and MOSES_TOPgc simulated similar soil wetness during this period, so only MOSES is shown. Similarly, MOSES_TOPsim was similar to MOSES_TOP.) In MOSES, the period of vegetation stress started a month earlier and lasted longer than with MOSES_TOP, with substantial impacts on the modeled evaporation (Fig.7b). Cumulative evaporation was 28% greater in MOSES_TOP over the period June to September 1984 while sensible heat was 31% lower (not shown). Differences of this magnitude would have substantial impact on an atmospheric model: if this average heat flux difference was assumed to occur over 12 hours of daytime and to diverge in a 1km deep boundary layer, the temperature difference would be ~1.3K.

Although all the TOPMODEL-based models were calibrated to give similar performance for runoff, their internal state variables often had rather different values. For example, during the period shown in Fig.7 the water table was on average 1.4m deeper in MOSES_TOPgc than in MOSES_TOP, as a result of differences in parameterization and parameter values. Although this difference was not significant to the present work, it could be important for other processes, for example trace gas emission over wetlands.

8. Discussion

When calibrated, both the PDM and TOPMODEL-type approaches perform better than the standard MOSES model which has no representation of subgrid soil moisture variability. The TOPMODEL-type approach is found to be superior over three catchments of the size of a typical gridbox in an atmospheric model. This is in agreement with the findings of *Warrach et al.*[2002] for a single, small catchment. The similar forms and results of the TOPMODEL-type parameterizations suggest that any of these models could be used, but this result will have to be confirmed for other

environments. The PDM and TOPMODEL-TYPE approaches have optimum parameter values that do not vary much for the three catchments studied, suggesting that detailed calibration may not be required for every catchment.

For models using a PDM-like approach, *Dumenil and Todini* [1992] and *Hagemann and Gates* [2003] have suggested how the parameters can be related to catchment characteristics, but these require further investigation and most studies have calibrated the parameters.

In principle, an attractive feature of TOPMODEL is that readily-available elevation data can be used to define an important input, namely the pdf of λ. However, many studies have shown that the pdf is sensitive to the resolution of the data, and so even the topographic parameters are uncertain. This uncertainty has led some to abandon or revise the use of λ in their models [*Niu et al.*, 2005; *Decharme et al.*, 2006]. In the present work, compensation between parameters meant that the importance of uncertainty in λ varied with the value of α. In the present study, the approach taken was to adjust Λ (broadly in line with that suggested by scaling studies) and calibrate α within the range suggested as physically reasonable. The robustness of this procedure will be investigated in future work. Users of TOPMODEL-type models must be aware of the uncertainty in λ and its possible impact on their model and its calibration.

Despite the large uncertainty in global fields of λ, there does appear to be useful information in this data. For example, our unpublished work shows significant correlations between HYDRO1K λ and observed extent of inundation. Thus although the absolute value of λ is uncertain, it might be possible to employ a relatively simple downscaling or correction method, and retain useful information about spatial variability.

The large uncertainty in parameter values for the models studied suggests that some calibration is currently essential for models of runoff generation. The need to calibrate a model is not necessarily a major obstacle to global implementation if, as was the case here, the model is not very sensitive to variations of parameter values around the optimum values. Further, *Gulden et al.* [2007] suggest that a suitable choice of hydrological parameterization can reduce the sensitivity of a

model to poor choices of uncertain parameter values, although which of the schemes tested here would fare best in that respect has not been examined.

Although it is tempting to relate all these models, and in particular those based on TOPMODEL, to processes that occur on the scale of a small catchment, they are all highly simplified representations of reality. Particularly at larger scales, the parameterizations may be better thought of as convenient functional forms that capture some of the essential dynamics of catchments.

9. Conclusions

The impact of different parameterizations of runoff generation in the MOSES land surface model was tested using observed streamflow from three mesoscale catchments. Parameterizations based on the Probability Distributed Model (PDM) and TOPMODEL were implemented. Runoff in the standard MOSES is dominated by drainage which varies too slowly to match the observed streamflow. MOSES_PDM added a representation of saturation excess surface runoff to the standard model, while the TOPMODEL-based models additionally altered the representation of subsurface runoff. After calibration, the alternative parameterizations performed considerably better than the standard model. The best results were found using any of the parameterizations based on TOPMODEL, which were better because they allowed the subsurface runoff to vary more quickly, with smaller volumes of surface runoff contributing to flow peaks. Although all the new models required extra calibration, a single set of parameter values was identified for each that could be used in all catchments with results comparable to those found from calibration. Attention was drawn to uncertainty in the value of the topographic index, which is an important parameter in TOPMODEL-type models. The simulation of turbulent fluxes during dry periods was sensitive to the choice of parameterization, which would be important when coupled to an atmospheric model.

Our future work aims to extend this work to other environments, and to investigate the use of catchment characteristics for estimating parameters *a priori*. We also intend to investigate the use of remote sensing products for the assessment of runoff parameterizations, particularly moisture stress [e.g. *Anderson et al.*, 2007], inundation and wetland extent [e.g. *Prigent et al.*, 2001] and changes in terrestrial water storage [e.g. *Niu et al.*, 2007].

Acknowledgements

This work was supported by the UK Natural Environment Research Council and the UK Department for Environment, Food and Rural Affairs under the Climate Prediction Programme PECD 7/12/37. The Rhone-AGG data, including the meteorological driving data, were provided by Météo-France, CNRM. Observations of streamflow were provided through the FRIEND project.

Appendix: The calculation of saturation excess surface runoff in MOSES_PDM

Given a rainfall rate P (net of interception) over a timestep of length Δt, the rate of saturation excess surface runoff (R_s) is found as

$$R_s \Delta t = P\Delta t + S - S_{\max} + (S_{\max} - S_o)\left[(1 - f_{sat})^{1/(b+1)} - \frac{P\Delta t}{(b+1)(S_{\max} - S_0)}\right]^{b+1}$$

for $P\Delta t > (1+b)(S_{\max} - S_0)(1 - f_{sat})^{1/(b+1)}$

$$R_s \Delta t = P\Delta t + S - S_{\max}$$

for $P\Delta t \le (1+b)(S_{\max} - S_0)(1 - f_{sat})^{1/(b+1)}$

where b, f_{sat}, S, S_{max} and S_o are as described in Section 2.2.

References

Anderson, M. C., J. M. Norman, J. R. Mecikalski, J. A. Otkin, and W. P. Kustas (2007), A climatological study of evapotranspiration and moisture stress across the continental United States based on thermal remote sensing: 2. Surface moisture climatology, *J. Geophys. Res. - Atmospheres*, *112*, D11112, doi:11110.11029/12006JD007507

Beven, K. (1982), On Subsurface Stormflow - an Analysis of Response-Times, *Hydrol. Sci. J.-J. Sci. Hydrol.*, *27*, 505-521

Beven, K. (1997), TOPMODEL: A critique, *Hydrological Processes*, *11*, 1069-1085

Beven, K. J., and M. J. Kirkby (1979), A physically based, variable contributing area model of basin hydrology, *Hydrolological Sciences Bulletin*, *24*, 43-69

Blyth, E. (2002), Modelling soil moisture for a grassland and a woodland site in south-east England, *Hydrology and Earth System Sciences*, *6*, 39-47

Boone, A., F. Habets, J. Noilhan, D. Clark, P. Dirmeyer, S. Fox, Y. Gusev, I. Haddeland, R. Koster, D. Lohmann, S. Mahanama, K. Mitchell, O. Nasonova, G. Y. Niu, A. Pitman, J. Polcher, A. B. Shmakin, K. Tanaka, B. van den Hurk, S. Verant, D. Verseghy, P. Viterbo, and Z. L. Yang (2004), The Rhone-aggregation land surface scheme intercomparison project: An overview, *J. Climate 17*, 187-208

Bormann, H. (2006), Impact of spatial data resolution on simulated catchment water balances and model performance of the multi-scale TOPLATS model, *Hydrology and Earth System Sciences*, *10*, 165-179

BRGM (1970), *Atlas des eaux souterraines de la France (Altas of groundwater in France)*, Bureau de Recherches Geologiques et Minieres, Paris.

Chen, J., and P. Kumar (2001), Topographic influence on the seasonal and interannual variation of water and energy balance of basins in North America, *J. Climate 14*, 1989-2014

Clapp, R. B., and G. M. Hornberger (1978), Empirical equations for some soil hydraulic properties, *Wat Resour Res*, *14*, 601-604

Decharme, B., H. Douville, A. Boone, F. Habets, and J. Noilhan (2006), Impact of an exponential profile of saturated hydraulic conductivity within the ISBA LSM: Simulations over the Rhone Basin, *Journal of Hydrometeorology*, *7*, 61-80

Dolman, A. J., and D. Gregory (1992), The parametrization of rainfall interception in GCMs, *Q. J. R. Meteorol. Soc.*, *118*, 455-467

Ducharne, A., R. D. Koster, M. J. Suarez, M. Stieglitz, and P. Kumar (2000), A catchment-based approach to modeling land surface processes in a general circulation model 2. Parameter estimation and model demonstration, *J. Geophys. Res. - Atmospheres*, *105*, 24823-24838

Dumenil, L., and E. Todini (1992), A rainfall-runoff scheme for use in the Hamburg climate model, in *Advances in theoretical hydrology, a tribute to James Dooge*, edited by J. P. O'Kane, pp. 129-157, Elsevier.

Essery, R. L. H., M. J. Best, R. A. Betts, P. M. Cox, and C. M. Taylor (2003), Explicit representation of subgrid heterogeneity in a GCM land surface scheme, *Journal of Hydrometeorology*, *4*, 530-543

Famiglietti, J. S., and E. F. Wood (1994), Multiscale Modeling of Spatially-Variable Water and Energy-Balance Processes, *Water Resources Research*, *30*, 3061-3078

1 Franchini, M., J. Wendling, C. Obled, and E. Todini (1996), Physical interpretation and sensitivity
2 analysis of the TOPMODEL, *J. Hydrol.*, *175*, 293-338

3 Gedney, N., and P. M. Cox (2003), The sensitivity of global climate model simulations to the
4 representation of soil moisture heterogeneity, *Journal of Hydrometeorology*, *4*, 1265-1275

5 Gulden, L. E., E. Rosero, Z. L. Yang, M. Rodell, C. S. Jackson, G. Y. Niu, P. J. F. Yeh, and J.
6 Famiglietti (2007), Improving land-surface model hydrology: Is an explicit aquifer model better
7 than a deeper soil profile?, *Geophysical Research Letters*, *34*, L09402,
8 doi:09410.01029/02007GL029804

9 Habets, F., J. Noilhan, C. Golaz, J. P. Goutorbe, P. Lacarrere, E. Leblois, E. Ledoux, E. Martin, C.
10 Ottle, and D. Vidal-Madjar (1999), The ISBA surface scheme in a macroscale hydrological model
11 applied to the Hapex-Mobilhy area - Part II: Simulation of streamflows and annual water budget, *J.*
12 *Hydrol.*, *217*, 97-118

13 Habets, F., and G. M. Saulnier (2001), Subgrid runoff parameterization, *Phys. Chem. Earth Pt B-*
14 *Hydrol. Oceans Atmos.*, *26*, 455-459

15 Hagemann, S., and L. D. Gates (2003), Improving a subgrid runoff parameterization scheme for
16 climate models by the use of high resolution data derived from satellite observations, *Climate*
17 *Dynamics*, *21*, 349-359

18 Ibbitt, R., and R. Woods (2004), Re-scaling the topographic index to improve the representation of
19 physical processes in catchment models, *J. Hydrol.*, *293*, 205-218

20 Koster, R. D., and P. C. D. Milly (1997), The interplay between transpiration and runoff
21 formulations in land surface schemes used with atmospheric models, *J. Climate 10*, 1578-1591

Koster, R. D., M. J. Suarez, A. Ducharne, M. Stieglitz, and P. Kumar (2000), A catchment-based approach to modeling land surface processes in a general circulation model 1. Model structure, *J. Geophys. Res. - Atmospheres*, *105*, 24809-24822

Kumar, P. (2004), Layer averaged Richard's equation with lateral flow, *Advances in Water Resources*, *27*, 522-532

Kumar, P., K. L. Verdin, and S. K. Greenlee (2000), Basin level statistical properties of topographic index for North America, *Advances in Water Resources*, *23*, 571-578

Liang, X., and Z. H. Xie (2001), A new surface runoff parameterization with subgrid-scale soil heterogeneity for land surface models, *Advances in Water Resources*, *24*, 1173-1193

Moore, R. J. (1985), The Probability-Distributed Principle and Runoff Production at Point and Basin Scales, *Hydrol. Sci. J.-J. Sci. Hydrol.*, *30*, 273-297

Moore, R. J., and V. A. Bell (2002), Incorporation of groundwater losses and well level data in rainfall-runoff models illustrated using the PDM, *Hydrology and Earth System Sciences*, *6*, 25-38

Nash, J. E., and J. V. Sutcliffe (1970), River flow forecasting through conceptual models. 1. A discussion of principles, *J. Hydrol.*, *10*, 282-290

Niu, G. Y., and Z. L. Yang (2003), The versatile integrator of surface atmospheric processes - Part 2: evaluation of three topography-based runoff schemes, *Global and Planetary Change*, *38*, 191-208

Niu, G. Y., Z. L. Yang, R. E. Dickinson, and L. E. Gulden (2005), A simple TOPMODEL-based runoff parameterization (SIMTOP) for use in global climate models, *J. Geophys. Res. - Atmospheres*, *110*, D21106, doi:21110.21029/22005JD006111

Niu, G. Y., Z. L. Yang, R. E. Dickinson, L. E. Gulden, and H. Su (2007), Development of a simple groundwater model for use in climate models and evaluation with Gravity Recovery and Climate Experiment data, *J. Geophys. Res. - Atmospheres*, *112*, D07103, doi:07110.01029/02006JD007522

Pradhan, N. R., Y. Tachikawa, and K. Takara (2006), A downscaling method of topographic index distribution for matching the scales of model application and parameter identification, *Hydrological Processes*, *20*, 1385-1405

Prigent, C., E. Matthews, F. Aires, and W. B. Rossow (2001), Remote sensing of global wetland dynamics with multiple satellite data sets, *Geophysical Research Letters*, *28*, 4631-4634

Saulnier, G. M., C. Obled, and K. Beven (1997), Analytical compensation between DTM grid resolution and effective values of saturated hydraulic conductivity within the TOPMODEL framework, *Hydrological Processes*, *11*, 1331-1346

Sivapalan, M., K. Beven, and E. F. Wood (1987), On Hydrologic Similarity .2. A Scaled Model of Storm Runoff Production, *Water Resources Research*, *23*, 2266-2278

Stieglitz, M., D. Rind, J. Famiglietti, and C. Rosenzweig (1997), An efficient approach to modeling the topographic control of surface hydrology for regional and global climate modeling, *J. Climate* *10*, 118-137

Warrach, K., M. Stieglitz, H. T. Mengelkamp, and E. Raschke (2002), Advantages of a topographically controlled runoff simulation in a soil-vegetation-atmosphere transfer model, *Journal of Hydrometeorology*, *3*, 131-148

Wolock, D. M., and G. J. McCabe (2000), Differences in topographic characteristics computed from 100- and 1000-m resolution digital elevation model data, *Hydrological Processes*, *14*, 987-1002

1 Wolock, D. M., and C. V. Price (1994), Effects of Digital Elevation Model Map Scale and Data
2 Resolution on a Topography-Based Watershed Model, *Water Resources Research*, *30*, 3041-3052

3 Wood, E. F., D. P. Lettenmaier, and V. G. Zartarian (1992), A Land-Surface Hydrology
4 Parameterization with Subgrid Variability for General-Circulation Models, *J. Geophys. Res. -*
5 *Atmospheres*, *97*, 2717-2728

6 Woods, R. A., and M. Sivapalan (1997), A connection between topographically driven runoff
7 generation and channel network structure, *Water Resources Research*, *33*, 2939-2950

8 Zhang, W. H., and D. R. Montgomery (1994), Digital Elevation Model Grid Size, Landscape
9 Representation, and Hydrologic Simulations, *Water Resources Research*, *30*, 1019-1028
10
11

Figure 1: Examples of 3-day average precipitation and streamflow for the Ain, during part of the validation period. (a) The components of precipitation. The scale on the right hand side shows the precipitation in terms of an equivalent streamflow rate. (b) streamflow as modelled by MOSES - this was almost all subsurface flow (c) streamflow as modelled by calibrated MOSES_PDM (d) surface and subsurface components of runoff from MOSES_PDM (e) as c but for calibrated MOSES_TOP (f) as d but for calibrated MOSES_TOP.

Figure 2: Efficiency for 3-day average flow during the validation period, comparing MOSES with modified versions of the model. Values are shown for three catchments, and the average over the catchments. For each, six models are compared. The first bar represents MOSES, the next three bars represent versions of MOSES_PDM, and the final two bars represent versions of MOSES_TOP. For MOSES_PDM, PDM_0 denotes a model with S_0=0, PDM_calib is the calibrated model for each catchment and PDM_best is the best overall model. The adjacent whiskers indicate the range given by varying S_0 ±10% about the best overall model. For MOSES_TOP, TOP_calib denotes the calibrated model for each catchment and TOP_best is the best overall model. The whiskers indicate the range given by varying f and α by ±10% about the best overall model.

Figure 3: Sensitivity of MOSES_PDM to parameter values, using data for the Ain from the validation period.

Figure 4: Published estimates of how the average topographic index changes with the resolution of the input data. Bracketed numbers in the legend give the range of resolution considered in each

study. The results for Ibbit and Woods (2004) are extrapolated down to 1m, using the relationship proposed in their Fig.9.

Figure 5: Sensitivity of MOSES_TOP to parameter values, using data from the Ain catchment in the validation period. (a) Sensitivity to α [with f=3] and f [with α=100]. Λ was given by its adjusted value Λ_{1000}-5 (b) Sensitivity to Λ with f=3, for four values of α. $\Delta\Lambda_{1000}$ is the difference from Λ_{1000}.

Figure 6: Autocorrelation of 3-day average flow in the Ain during the validation period, for observed and modelled flows.

Figure 7: Modelled 5-day averages for the Ardeche, as simulated by MOSES and MOSES_TOP. (a) Soil wetness in the top 1m as a fraction of saturation. The dashed line shows the wetness above which transpiration is not restricted by soil water. (b) Soil evaporation (transpiration plus evaporation from the soil surface).

TABLE 1: Statistics of the catchments. Elevation statistics were calculated from HYDRO1K data. The runoff ratio is the ratio of streamflow to precipitation. Precipitation and runoff ratio are for August 1986-July 1989. The runoff ratio for the Ardeche is for August 1987-July 1989.

	Area (km^2)	Average elevation (m)	Standard deviation of elevation (m)	Precipitation (mm)	Runoff ratio
Ain at Vouglans	1120	742	198	1699	0.81
Ardeche at Sauze St Martin	2240	571	364	1430	0.64
Ognon at Pesmes	2040	336	120	1275	0.47

1 TABLE 2: Statistics of the streamflow observed and modeled by MOSES for August 1986 to July

2 1989, calculated using three-day averaged flow.

	Observed mean flow (m^3 s^{-1})	Bias (%)	Mean absolute error (%)	Efficiency
Ain	42.3	3	53	0.50
Ardeche	64.8	-4	42	0.64
Ognon	37.4	25	46	0.65

3

TABLE 3: Values of the calibrated parameters and model efficiency (E) during the validation period, for MOSES_PDM. b is the shape factor, S_0 is the soil water storage below which there is no surface runoff and S_{max} is the maximum possible gridbox soil water storage. Model versions were PDM_0 (with S_0=0) and PDM_calib (calibrated for each catchment). Overall best denotes the single set of parameter values that gave best results when used for all catchments, and the E value is the average over the catchments.

	PDM_0		PDM_calib		
	b	E	S_0/S_{max}	B	E
Ain	0.25	0.67	0.75	10	0.75
Ardeche	0.25	0.79	0.75	10	0.88
Ognon	0.0	0.65	0.75	0.5	0.69
Overall best	0.0	0.60	0.75	10	0.78

TABLE 4: Values of the calibrated parameters and model efficiency (E) during the validation period, for versions of MOSES with TOPMODEL-type parameterizations. f is the decay coefficient for saturated hydraulic conductivity, α is the anisotropy, which was allowed to vary between 1 and 100, and R_{bmax} is the subsurface flow rate for water table depth of zero. Overall best denotes the single set of parameter values that gave best results when used for all catchments, and the E value is the average over the catchments. Overall best is also shown for runs with MOSES_TOP in which α was allowed to vary between 1 and 2000.

	MOSES-TOP			MOSES-TOPgc			MOSES-TOPsim		
	f (m^{-1})	α	E	f (m^{-1})	α	E	f (m^{-1})	R_{bmax} (10^{-3} kg m^{-2} s^{-1})	E
Ain	3.0	100	0.87	7.0	100	0.87	3.0	0.8	0.89
Ardeche	3.0	75	0.87	4.5	75	0.90	3.0	1.0	0.84
Ognon	2.5	100	0.76	3.5	100	0.81	2.5	1.0	0.79
Overall best	3.0	100	0.81	4.5	100	0.84	3.0	1.0	0.82
Overall best ($\alpha \leq 2000$)	3.5	2000	0.85	-	-	-	-	-	-

TABLE 5: Summary of performance of each model during the validation period. All runs used the "best overall" parameters for the model, i.e. the same parameters were used in all catchments. "Average" is the average over all catchments.

		MOSES	MOSES-PDM	MOSES-TOP	MOSES-TOPgc	MOSES-TOPsim
Efficiency	Ain	0.50	0.75	0.87	0.87	0.89
	Aredeche	0.64	0.88	0.88	0.90	0.84
	Ognon	0.65	0.71	0.69	0.75	0.76
	Average	0.60	0.78	0.81	0.84	0.83
Bias (%) (model-observed)	Ain	+2.8	+2.5	-3.4	-1.7	-0.0
	Aredeche	-3.7	-3.6	-8.1	-4.0	-8.5
	Ognon	+25.4	+25.4	+21.3	+21.3	+21.9
	Average of absolute values	+10.6	+10.5	+11.0	+9.0	+9.5
MAE (%)	Ain	53	37	25	26	23
	Aredeche	42	29	24	25	26
	Ognon	46	42	35	33	33
	Average	47	36	28	28	27

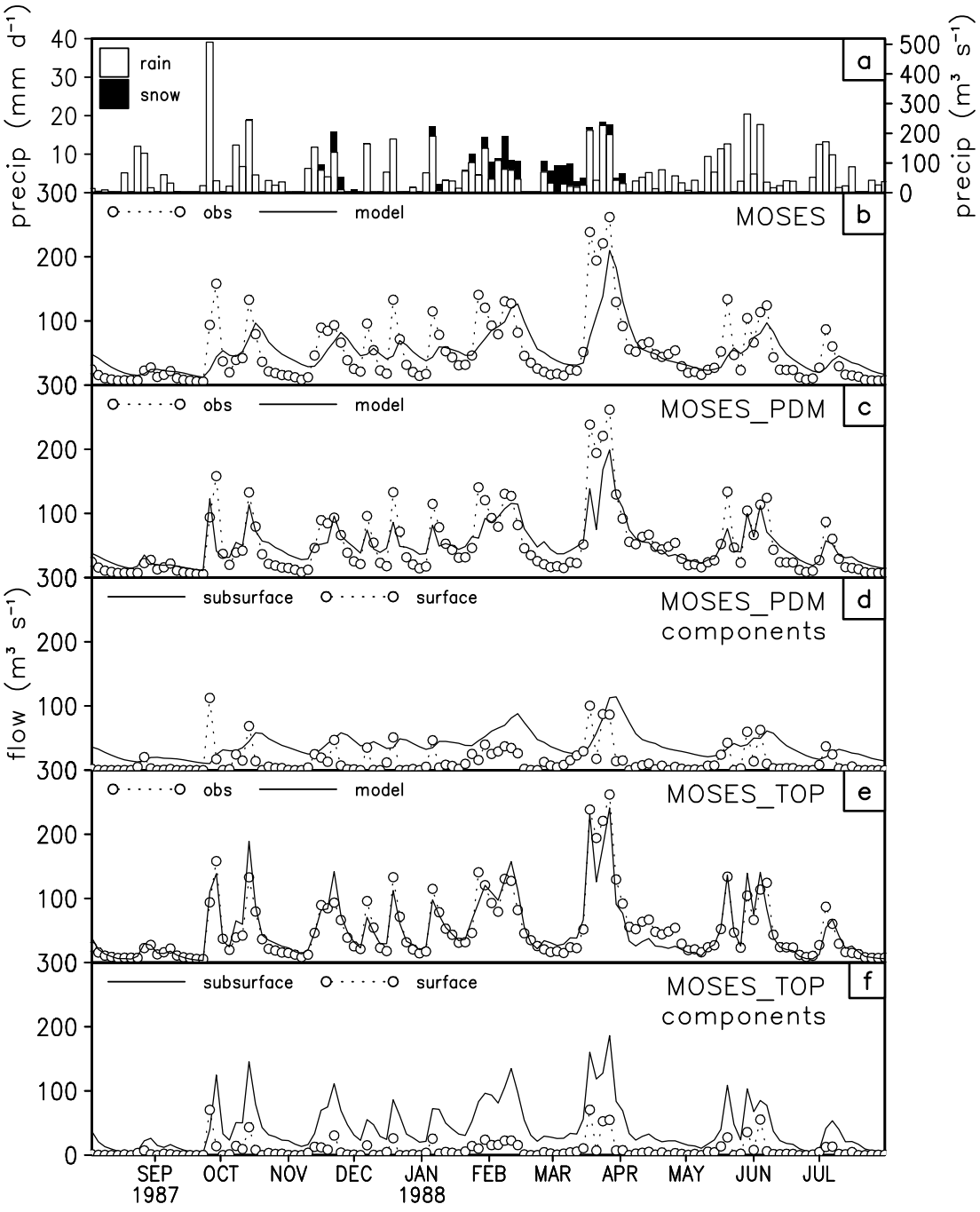

Figure 1: Examples of 3-day average precipitation and streamflow for the Ain, during part of the validation period. (a) The components of precipitation. The scale on the right hand side shows the precipitation in terms of an equivalent streamflow rate. (b) streamflow as modelled by MOSES - this was almost all subsurface flow (c) streamflow as modelled by calibrated MOSES_PDM (d) surface and subsurface components of runoff from MOSES_PDM (e) as c but for calibrated MOSES_TOP (f) as d but for calibrated MOSES_TOP.

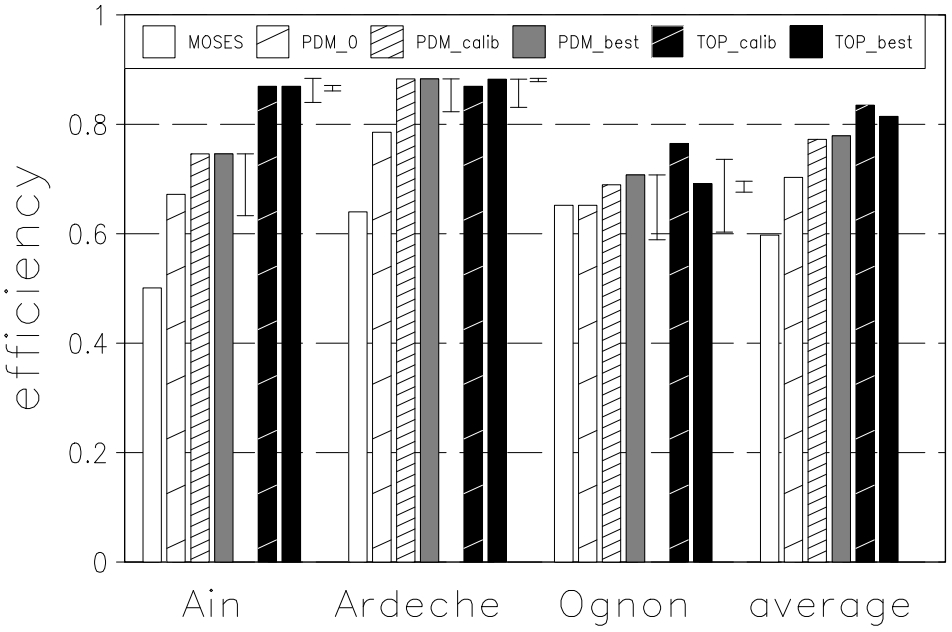

Figure 2: Efficiency for 3-day average flow during the validation period, comparing MOSES with modified versions of the model. Values are shown for three catchments, and the average over the catchments. For each, six models are compared. The first bar represents MOSES, the next three bars represent versions of MOSES_PDM, and the final two bars represent versions of MOSES_TOP. For MOSES_PDM, PDM_0 denotes a model with S_0=0, PDM_calib is the calibrated model for each catchment and PDM_best is the best overall model. The adjacent whiskers indicate the range given by varying S_0 by ±10% about the best overall model. For MOSES_TOP, TOP_calib denotes the calibrated model for each catchment and TOP_best is the best overall model. The whiskers indicate the range given by varying f and α by ±10% about the best overall model.

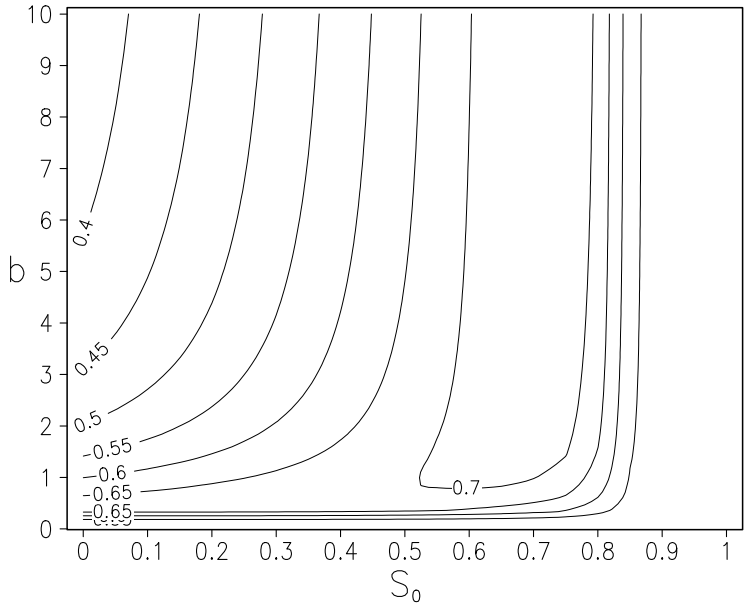

Figure 3: Sensitivity of MOSES_PDM to parameter values, using data for the Ain from the validation period.

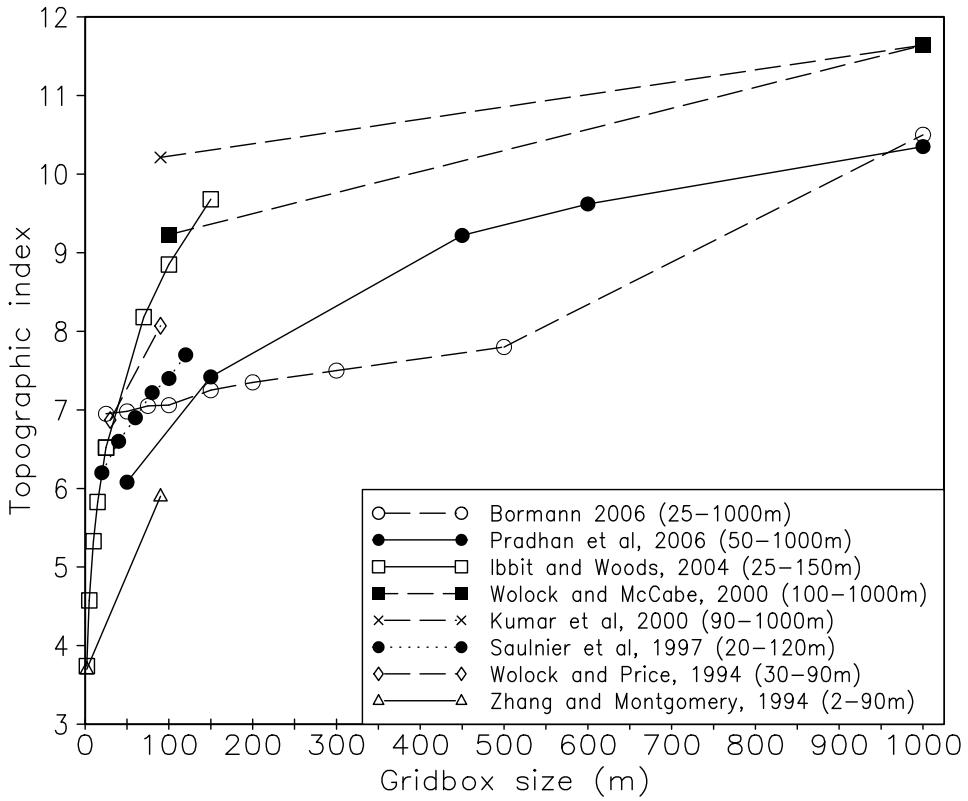

Figure 4: Published estimates of how the average topographic index changes with the resolution of the input data. Bracketed numbers in the legend give the range of resolution considered in each study. The results for Ibbit and Woods (2004) are extrapolated down to 1m, using the relationship proposed in their Fig.9.

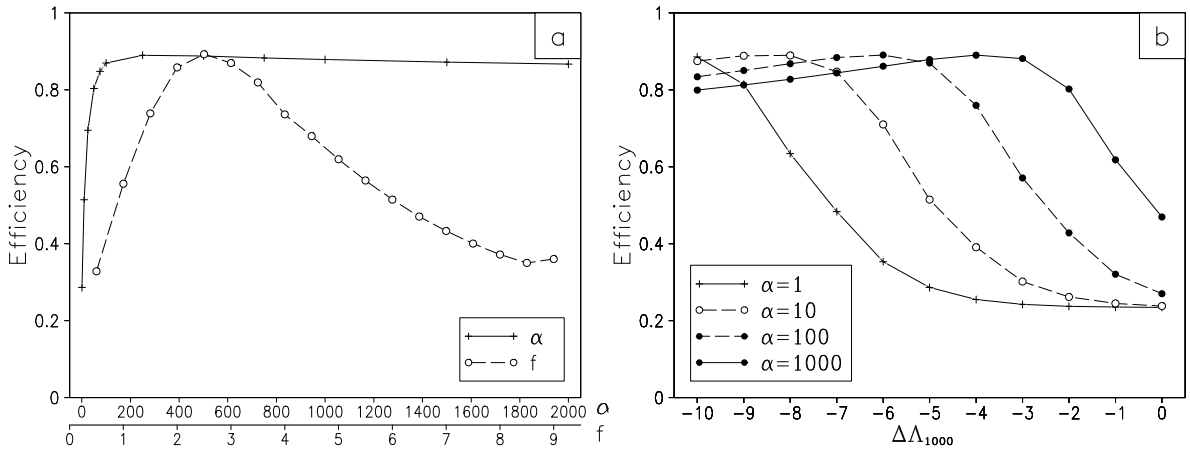

Figure 5: Sensitivity of MOSES_TOP to parameter values, using data from the Ain catchment in the validation period. (a) Sensitivity to α [with f=3] and f [with α=100]. Λ was given by its adjusted value $\Lambda_{1000} - 5$ (b) Sensitivity to Λ with f=3, for four values of α. $\Delta\Lambda_{1000}$ is the difference from Λ_{1000}.

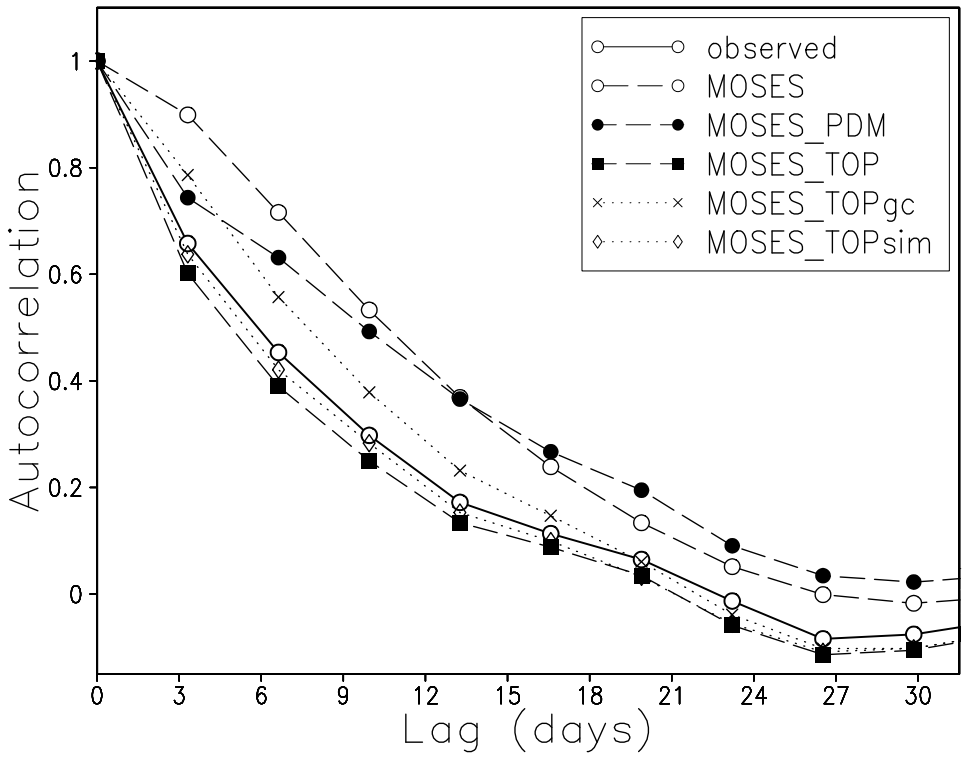

Figure 6: Autocorrelation of 3-day average flow in the Ain during the validation period, for observed and modelled flows.

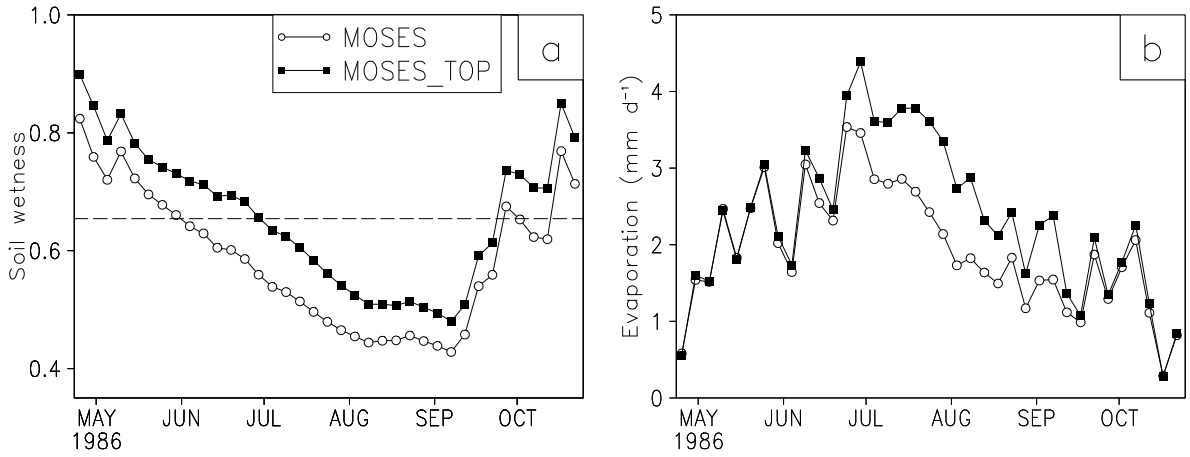

Figure 7: Modelled 5-day averages for the Ardeche, as simulated by MOSES and MOSES_TOP.(a) Soil wetness in the top 1m as a fraction of saturation. The dashed line shows the wetness above which transpiration is not restricted by soil water. (b) Soil evaporation (transpiration plus evaporation from the soil surface).